Polymerization study and rheological behavior of a RTM6 epoxy resin system during preprocessing step

Nicolas Causse · Stephanie Benchimol · Lilian Martineau · Delphine Carponcin · Antoine Lonjon · Mathieu Fogel · Jany Dandurand · Eric Dantras · Colette Lacabanne

Abstract Curing process and rheological behaviors of a monocomposant epoxy resin used in structural aeronautic applications are investigated. This study helped settle the basic parameters in order to optimize the infusion process of carbon fibers in an epoxy matrix. The effect of carbon nanotube dispersion during the preinjection step is also studied to improve electrical behavior of composite parts. The curing process has been analyzed at isothermal temperature using differential scanning calorimetry technique. Viscosity measurements were achieved with a Couette geometry, suitable for low viscosity resin. A shear-thinning effect caused by adding CNTs in the epoxy matrix is detected. It is more pronounced at high temperature for increasing CNT mass content.

Keywords Epoxy resin · Curing · Shear viscosity · Carbon nanotubes · Nano composites

Introduction

Development of light multi-functional materials represents one of the most important challenges for aeronautic and space industries. Carbon fiber-reinforced polymer composites (CFRP) are increasingly used to reduce the structure mass. Introduction of inorganic charges is an extrinsic way for adding new functionalities to these materials (electrical or thermal conductivity, damping, etc.).

One of the most relevant examples is the electrical conductivity level of composites. In spite of the intrinsic electrical conductivity of carbon fibers, composites have a poor conductivity in its perpendicular plan direction [1]. The inter-laminar epoxy layer electrically insulates the successive carbon fiber layers. This low conductivity makes composite structures more vulnerable to withstand lightning strikes and unable to prevent electrostatic accumulation. It is therefore necessary to increase the electrical conductivity of the epoxy matrix to improve the transversal conductivity across the composite section.

Carbon nanotubes are particles with a high aspect ratio ($\xi \sim 1{,}000$) [2]. They are likely to improve the conductivity level of the inter-laminar epoxy layer [3]. They provide the same level of conductivity [4] as an epoxy resin filled with carbon black [5]. Due to their high aspect ratio, this value is obtained for a very low mass fraction (<0.5 mass%) [6]. This very low rate maintains the mechanical properties of epoxy matrix for a relatively small mass gain [7].

In order to manufacture filled CFRP using state of the art infusion processes (resin transfer molding, resin transfer infusion, etc.), some challenges have to be overcome. Indeed, the change in thermoset resin properties due to the insertion of charges must be considered [8–10]. The incorporation and dispersion of charges must be achieved before the injection process. The influence of this new step during the part manufacturing process must be evaluated: The duration and temperature of dispersion step should alter the polymerization process. Moreover, particles enhance largely the viscosity for very low rate of fillers [11], which can affect the injection step.

RTM6 has been chosen for this study because it is an epoxy resin largely used in the manufacturing of carbon

N. Causse · S. Benchimol · L. Martineau · A. Lonjon · M. Fogel · J. Dandurand · E. Dantras (✉) · C. Lacabanne
Physique des Polymères, Institut Carnot CIRIMAT, Université de Toulouse, 31062 Toulouse, France
e-mail: eric.dantras@univ-tlse3.fr

D. Carponcin
IRT Saint Exupery MRV, 118, route de Narbonne, CS 44248, 31432 Toulouse, France

fiber-reinforced composites for aeronautic and space industries. This resin is especially suitable for resin transfer molding (RTM) process. Its manufacturer recommends preheating and injection at 80 °C to decrease its viscosity and facilitate the flow during injection. For this reason, the particle dispersion should be achieved just before injection during this preheating step. Then, the resin is cured in mold at higher temperature, and a post-curing step can be achieved to increase performances [12]. The curing process has already been studied by calorimetric, volumetric, dielectric, and optical techniques for curing temperatures proposed by manufacturer [13–17]. No study of the curing process during the preheating step at 80 °C has been achieved.

Understanding the polymerization process and rheological behavior of an existing commercial epoxy system is crucial [18]. Firstly, it is important to determine the influence of the dispersion step on the polymerization and the time available before injection. Secondly, we need to assess the rheological behavior of this resin and the influence of charges on it.

Experimental

Materials

The epoxy matrix used in this study is the commercially available RTM6 provided by Hexcel. This epoxy matrix is called a single-component resin: The epoxy prepolymer and amine hardener are already mixed together and degassed. Before studying it, resin was stored at −20 °C to freeze the macromolecular chains mobility and avoid curing reactions. It is typically used to manufacture structural composite parts using vacuum assisted resin transfer molding (thanks to a low viscosity at processing temperatures) and is usually cured at 180 °C.

The carbon nanotubes selected for this study are multiwalls carbon nanotubes (MWCNT: walls 5–15, diameter 10–15 nm, length 0.1–10 µm) provided by Arkema (France). A masterbatch based on Cytec's MVR 444 resin was prepared by Arkema using their Graphistrength C S1-25 MWCNTs as an additive. The CNT masterbatch is diluted in the RTM6 resin to the final CNT concentration. The dispersion is achieved at 80 °C by an ultrasonic apparatus (1 min), corresponding to a dissipated power of 300 W.

Analysis techniques

Differential scanning calorimetry

The curing process was investigated using a TA Instruments 2920 differential scanning calorimeter (DSC). Experiments were performed on a constant amount of resin (15 mg). All the DSC measurements were taken under helium atmosphere. The glass transition was taken as the midpoint of the heat capacity step during the heating. The residual heats of reaction (ΔH_r) were estimated using the area under the residual exotherm associated with curing reaction in the DSC scans. The baseline is determined between the onset and the end of the polymerization peak. Temperature scanning measurements from −50 to 350 °C (heating rate 10 °C min^{-1}) have been taken in order to measure the total reaction enthalpy $\left(\Delta H_r^{total}\right)$ and the glass transition temperature of the uncured epoxy (T_{g0}). Five samples have been analyzed to test the reproducibility.

Several samples were placed at 80 °C in an oven for various durations, until no additional curing can be detected (up to 140 h). Samples are then scanned from −50 to 350 °C at 10 °C min^{-1} in the calorimeter to determine the glass transition temperature (T_g) and the residual enthalpy of reaction $\left(\Delta H_r^t\right)$, that is, the heat evolved during completion of cross-linking at a curing time t. This analysis method has been preferred due to the slow polymerization kinetic expected for a low temperature curing process [19].

Rheological behavior analysis

The rheological behavior of the unfilled and filled epoxy polymer was studied using an ARES rheometer from TA Instruments. A so-called Couette test setup was employed. The Couette geometry used includes a cup containing the sample and applying the shear forces (lower part, linked to the motor) and a bob linked to the torque sensor (upper part). Parameters of the setup geometry include a gap of 1 mm between the lower and upper part, the upper cylinder having a diameter of 32 mm and a fully immersed length of 34 mm. This specific test setup was chosen in order to achieve a larger surface of contact with the sample, which enables a more appropriate range of torques to be measured by the sensor device (low viscosity of the resin at processing temperatures). Furthermore, the amount of material being tested remains the same all along the measurement (5 mL), which is not always the case with other geometries (for example: parallel plates).

Results and discussion

Polymerization study

The thermodynamic study of the polymerization evolution is performed by DSC. The resin is warmed up to 80 °C and placed in aluminum pan. Then, samples are analyzed after various polymerization durations. Figure 1 shows the scan

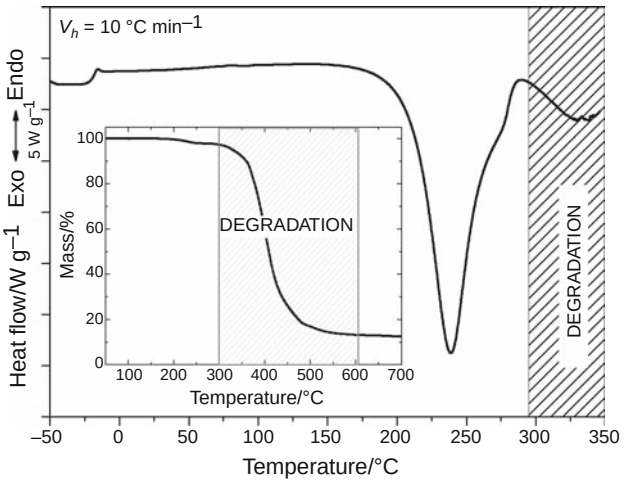

Fig. 1 DSC and TG scans of uncured RTM6 resin. The scan rate is 10 °C min^{-1} and sample mass is 15 mg

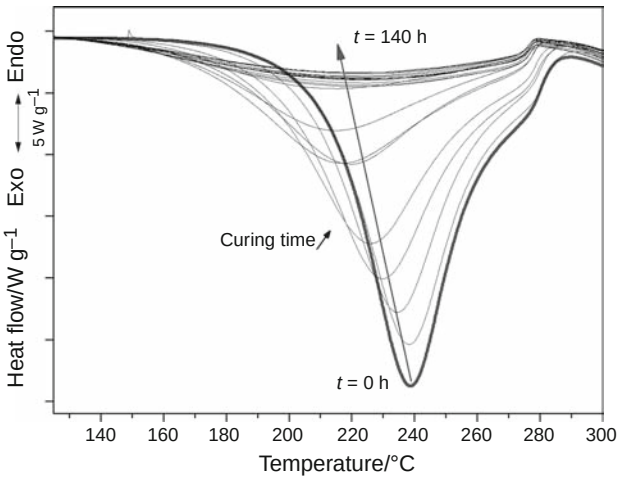

Fig. 2 Scans obtained for various curing durations at an isothermal temperature of 80 °C. The scan rate is 10 °C min^{-1}

at $t = 0$, that is, the scan of the uncured resin. The uncured resin exhibits a glass transition T_g at -17.5 ± 1 °C and an exothermic peak associated with curing reaction with a minimum at 238 ± 1 °C. The residual enthalpy ΔH_r^{total} is 391 ± 12 J g^{-1}. It is closely related to the complete conversion of reactive species. The beginning of RTM6 thermal degradation has been evaluated around 300 °C by thermogravimetry analysis (results not reported here for the purpose of clarity). The "degradation range" is reported on Fig. 1 (hatched area: determined by thermogravimetry (TG) analysis on the inserted graphic on Fig. 1). It shows that polymerization peak is not influenced by thermal degradation phenomena.

Firstly the polymerization is investigated through the residual enthalpy analysis, then using the glass transition temperature. Analogies between the two parameters are discussed in the third part.

Enthalpy of the reaction

Scans (focused on the polymerization peak) obtained for increasing polymerization times are shown in Fig. 2. The peak area decreases and its minimum is shifted to lower temperatures when the curing duration at 80 °C increases. The peak area represents the residual enthalpy of reaction ΔH_r^t after a curing time t, that is, the conversion of unreacted species due to heating ramp in DSC apparatus. The corresponding enthalpy of reaction after a curing time t can be calculated by subtracting the residual enthalpy of reaction ΔH_r^t after a curing time t to the total enthalpy of reaction ΔH_r^{total} (uncured resin). These parameters are used in Eq. 1 to calculate the conversion degree.

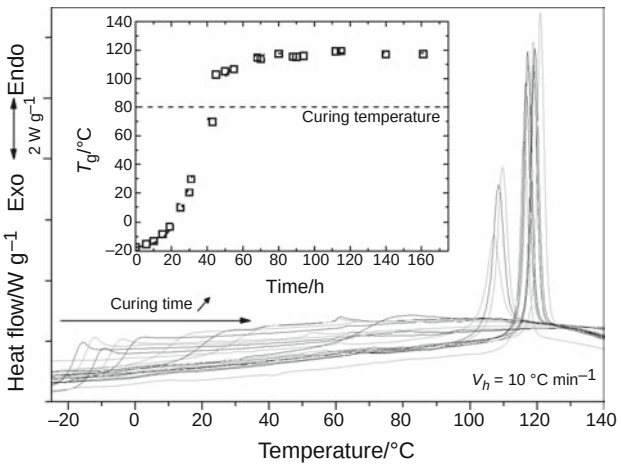

Fig. 3 RTM6 DSC scans and glass transition temperature as a function of curing duration at an isothermal temperature of 80 °C for neat epoxy resin

Glass transition temperature

The polymerization progress can also be characterized by monitoring the shift of the glass transition temperature. Scans (centered on the glass transition temperature region) obtained for increasing polymerization times are shown in Fig. 3. The T_g values as a function of curing time are also reported as insert. The glass transition temperature increases when the duration at 80 °C increases. Considering estimated reproducibility on T_g values, the T_g value does not evolve during the first 5 h of curing. This value increases by 4 °C between 5 and 10 h. Then, the T_g keeps going up according to two different steps. When T_g is lower

than the curing temperature, we note a strong and fast increase in T_g. As the T_g increases, it reaches the point where it comes above the isothermal temperature ($T_g > 80$ °C). As soon as this point is reached, the increase in T_g slows down. Moreover, an intense endothermic peak is superimposed to the heat flow signal associated with the glass transition temperature. This peak appears upon the sigmoidal change. The amplitude and the maximum temperature of this peak increase with an increasing curing time. It is associated with physical ageing phenomena and will be discussed in the next section.

Conversion degree

The determination of the residual enthalpy of reaction ΔH_r^t after a curing time t enables the evaluation of the conversion degree $\alpha_t^{\Delta H}$ as a function of time through Eq. 1.

$$\alpha_t^{\Delta H} = \frac{\Delta H_r^{\text{total}} - \Delta H_r^t}{\Delta H_r^{\text{total}}}, \tag{1}$$

where $\Delta H_r^{\text{total}}$ is the total enthalpy of reaction (uncured resin).

The conversion degree α_t^{Tg} can also be determined using the value of glass transition temperature T_{gt} after a curing time t (Eq. 2) [20]

$$\frac{T_{g_t} - T_{g_0}}{T_{g_\infty} - T_{g_0}} = \frac{\lambda \times \alpha_t^{Tg}}{1 - (1-\lambda)\alpha_t^{Tg}}, \tag{2}$$

where T_{g0} is the glass transition of uncured resin, $T_{g\infty}$ is the glass transition of a fully cured resin (i.e., conversion degree of 1 for a 1:1 stoichiometry) and λ is a parameter associated with the network structure. λ can be approached by $\frac{\Delta C_{p_\infty}}{\Delta C_{p_0}}$ where ΔC_{p_∞} and ΔC_{p_0} are the specific heat capacity increments of the fully cured and uncured resin, respectively. $T_{g\infty}$ and ΔC_{p_∞} cannot be determined in these curing conditions, and we used a literature value of $T_{g\infty} = 220$ °C [14] which is in a good agreement with another study on the same resin [15]. We treated ΔC_{p_∞} as an adjustable parameter $\left(\Delta C_{p_\infty} = 0.18 \pm 0.01\,\text{J g}^{-1}\,\text{K}^{-1}\right)$.

The conversion degrees determined by the two methods are plotted on Fig. 4 as a function of curing duration. The solid lines are used in this figure to facilitate methods comparison. The evolutions of conversion degree are very similar, whatever the determination way. During the first 10 h at 80 °C, the conversion degree is quite constant and close to zero. After a curing time of 10 h, it increases quickly to reach a value of 0.6 after 40 h. As most of epoxy systems [21, 22], the exothermic chemical reaction of polyaddition between amine groups and oxirane functions of epoxy resin changes the viscous resin with a low-molar

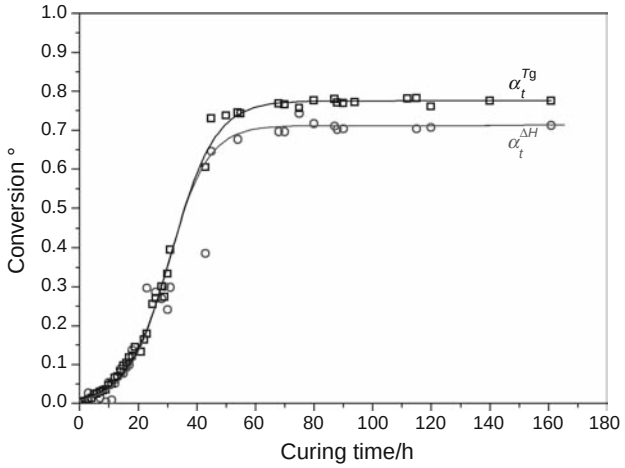

Fig. 4 Conversion degree $\alpha_t^{\Delta H}$ (from residual enthalpy) and α_t^{Tg} (from glass transition temperature) as a function of curing duration at 80 °C. The *solid lines* are guides to compare the evolutions of the two conversion degrees

mass into an amorphous viscoelastic solid. At the end of this cross-linking reaction, the three-dimensional network exhibits a quasi-infinite molar mass. Two steps can be identified during polymerization: gelation and vitrification. Gelation is the irreversible formation of an infinite macromolecular network. Vitrification occurs when the glass transition temperature increases up to the curing temperature. When polymerization goes up in the vitreous state, the reaction rate is significantly slowed down. In the present study of the influence of injection temperature (80 °C), the increase in conversion degree significantly slows down after 40 h due to vitrification (T_g becomes higher than 80 °C). Then, the conversion degree reaches a maximum value after 60 h: The reaction does not evolve anymore. This maximum depends on the parameter used to calculate α_t: It is about 0.71 for $\alpha_t^{\Delta H}$ and 0.77 for α_t^{Tg}.

The slight difference between these two maximum values may be explained in terms of physical ageing. Physical ageing [23–26] is associated with the instability (non-equilibrium state) of amorphous materials in the glassy state. At a temperature just above T_g, molecular segmental rearrangements remain possible and lead to a variation in molecular mobility as well as free volume of the polymer to reach the equilibrium thermodynamic state. Properties controlled by these two parameters are therefore affected. The endothermic peak superimposed on T_g during DSC experiments (see Fig. 3) is a manifestation of these phenomena. Just after vitrification, when the T_g becomes higher than 80 °C, we can observe physical ageing phenomena increasing with time. They can involve a slight increase in T_g and therefore in the value of α_t^{Tg}.

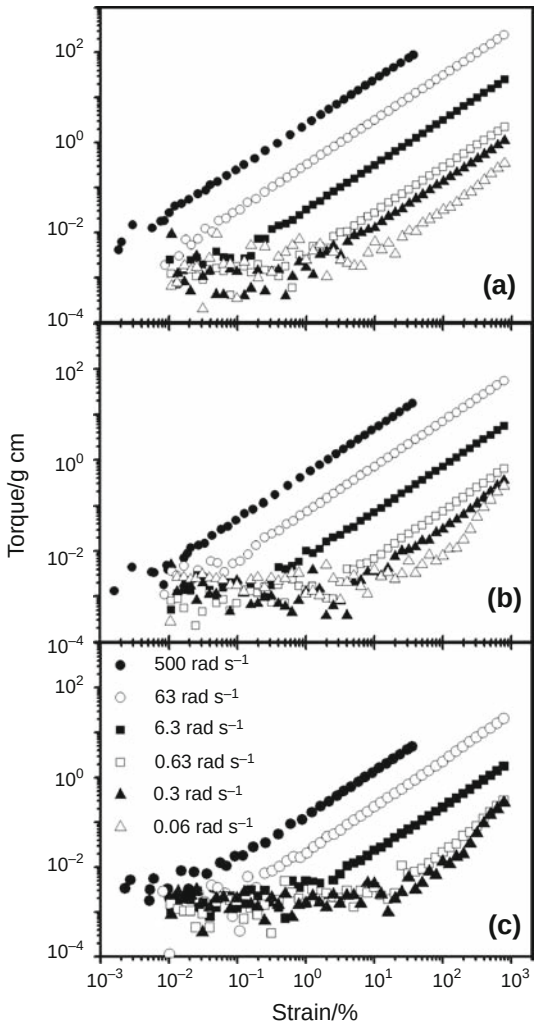

Fig. 5 Torque measured as a function of the strain applied for neat epoxy resin at **a** 60 °C, **b** 80 °C, and **c** 100 °C

Rheological behavior

In this section, the rheological behavior of the uncured epoxy is studied. The duration of all the tests does not exceed 1 h, negligible compared to 10 h (see previous section) in order to avoid any evolution due to beginning of polymerization process (i.e., it can be assumed that $\alpha \approx 0$ during all the measurements).

Influence of temperature on the shear flow properties of the RTM6 epoxy resin

Linear response domain First of all, the linear response domain of the resin with the applied strain must be experimentally determined for each considered temperature. Strain sweeps are performed isothermally in a range of strains from 10^{-2} to 8×10^{2} % (Fig. 5). These measurements are completed for a few selected shearing frequencies: 10^{-2}; 5.10^{-2}; 10^{-1}; 1; 10; 80 Hz. The linear response is observed in the torque evaluation. The aim is to determine the frequency domain for which the material exhibits a linear response to the stress applied: i.e., a requirement to determine the complex viscosity. Three temperatures (60, 80, and 100 °C) are tested in order to evaluate the effect of a slight process temperature variation.

Whatever the isotherm, the measured torque values are erratic for the lowest strains. For higher strains, they increase linearly when the strain increases. The dispersion can be explained by the low viscosity of RTM6 resin: For low strains and low angular frequencies ω, the rheometer torque sensor is under its sensitivity range (torque < 0.01 g cm). For 0.3 rad $s^{-1} \leq \omega \leq 63$ rad s^{-1}, the amplitude of linear response domain increases with angular frequency. At 500 rad s^{-1}, this amplitude decreases because for this high frequency, the rheometer cannot apply strain higher than 40 %. The amplitude of linearity response domain also decreases when the temperature increases. It is due to a decrease in resin viscosity involving the lack of rheometer sensitivity for low torque values. The best compromise allowing the largest frequency range is obtained for a 30 % strain for each considered temperature.

Shear viscosity In a second time, the rheological behavior is investigated as a function of shear frequency. Frequency sweeps are performed at the selected isothermal temperatures (60, 80, and 100 °C) for the selected strain (30 %, i.e., in the linear response domain of the material). In these conditions, the real part of the complex viscosity (η') can be determined (called dynamic viscosity on Fig. 6). For the low angular frequencies, as observed on previous section, dynamic viscosity exhibits an uncertainty due to torque sensor sensitivity. These erratic values are not considered. Depending on isothermal temperature, the dynamic viscosity becomes constant for different angular frequency ranges. Lower limits of these angular frequency ranges are, respectively, 0.1, 1, and 3 rad s^{-1} for 60, 80, and 100 °C temperature. At 60 °C, the dynamic viscosity reaches a constant value of 0.79 Pa s. At 80 °C, it is 0.18 Pa s and at 100 °C, 0.06 Pa s. Viscosity is temperature-dependent: It increases as the temperature decreases. This plateau is characteristic of a Newtonian fluid behavior: The viscosity does not depend on the angular frequency. The value at 80 °C is slightly lower than the one find in a previous study [15] (about 0.40 Pa s) and measured, thanks to parallel plate, probably due to this test geometry difference and the ability to keep the low viscosity fluid between the plates.

Above an angular frequency called ω_c, the dynamic viscosity decreases when the angular frequency increases. The angular frequency ω_c is a function of temperature: It decreases when temperature increases. The shear frequency dependence of viscosity is a characteristic shear-thinning

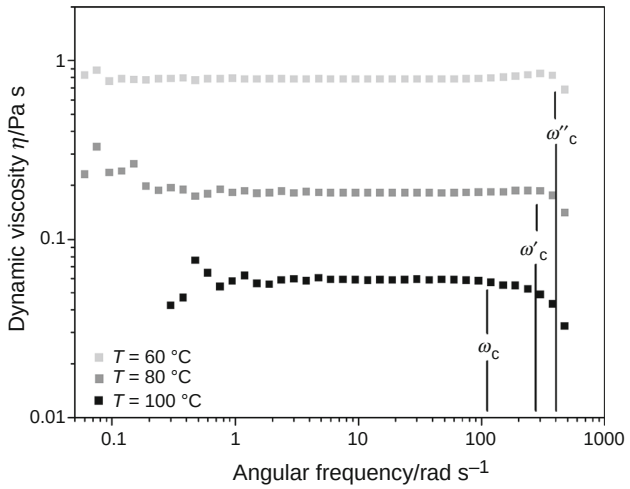

Fig. 6 Dynamic viscosity as a function of logarithmic angular frequency for neat epoxy resin at **a** 60 °C, **b** 80 °C, and **c** 100 °C

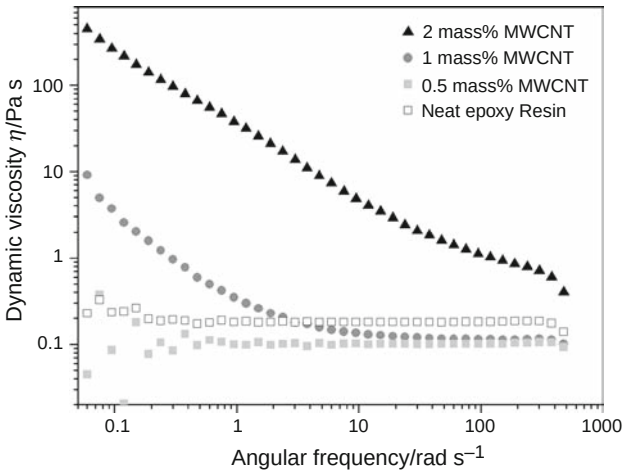

Fig. 7 Dynamic viscosity at 80 °C as a function of logarithmic angular frequency for neat epoxy resin and for CNT-modified resin loaded at 0.5, 1, and 2 mass% of MWCNT

behavior. It is not imputable to the test parameters because the linearity between torque and shear strain is respected (see Fig. 5, curves at 500 rad s^{-1}). A possible explanation is a local temperature elevation due to the strong strain applied on the resin by Couette cylinders. The variation of ω_c with test temperature can be explained by the viscosity temperature dependence. At high temperature, the low viscosity involves a higher friction between resin and Couette cylinders: The viscosity fall occurs for a lower angular frequency.

Influence of MWCNTs on the shear flow properties of the RTM6 epoxy resin

Evolution with MWCNT concentration Three mass fractions of CNTs have been introduced into the RTM6 resin to study the influence of carbon fillers on the rheological behavior. Figure 7 represents the dynamic viscosity as a function of angular frequency for epoxy resin filled from 0 to 2 mass% CNTs (strain of 30 %). Rheological behavior of the epoxy/0.5 mass% CNT composite is very close to neat resin one: a Newtonian plateau is observed from 0.5 to 300 rad s^{-1}. For higher angular frequency, a shear-thinning behavior is again observed, in the same way as the neat resin for $\omega > \omega_c$. The dynamic viscosity is about 0.11 Pa s. The slight difference (about 0.07 Pa s) of the viscosity value with neat resin is attributed to a dilution effect by the epoxy resin in the epoxy/CNT masterbatch. This resin exhibits a viscosity measured at 80 °C on a Couette geometry slightly lower than the RTM6 resin [27]. The epoxy/1 mass% CNT composite shows an initial viscosity of 10 Pa s (i.e., measured at the lowest angular frequency). In that case, the dynamic viscosity decreases with angular frequency to reach a plateau. This Newtonian plateau perfectly fits with the epoxy/0.5 mass% CNT composite. This dispersion presents a twofold behavior: This is initially shear thinning followed by a Newtonian at higher angular frequencies. The epoxy/0.5 mass% CNT composite viscosity decreases with angular frequency. It never reaches a plateau even if it approaches the one of other studied dispersions.

The shear-thinning behavior can be explained by the presence of interconnected carbon nanotube aggregates, induced by dispersion or by low shear conditions. Increasing strains result in a reduction in the size of aggregates and can lead to a complete dispersion of the aggregates [28]. When aggregates are not observed (functionalized CNT) some authors explain this behavior by the CNTs alignment in the flow direction [29].

Evolution with temperature The temperature influence on rheological behavior of epoxy resin/1 mass% CNTs dispersion is investigated on Fig. 8. The viscosity is not affected by the temperature for a low angular frequency. However, for higher frequencies, the viscosity becomes temperature-dependent: The shear-thinning behavior is amplified by an increase in temperature. At 60 °C, the resin exhibits a Newtonian plateau for a dynamic viscosity of 0.48 Pa s. This viscous behavior is modified by the temperature raise. Indeed, at 80 °C, the dynamic viscosity falls to 0.12 Pa s for a 50 rad s^{-1} angular frequency. At 100 °C, the viscosity continuously decreases all over the angular frequency range. At 60 °C, the high viscosity of epoxy matrix reduces the CNT mobility: The formation of a network of aggregates is limited. An increasing angular frequency does not change their dispersion. This behavior is similar to the one observed for a low rate of CNTs (0.5 %). The epoxy matrix viscosity increases with the temperature. The CNTs mobility release and the increasing angular frequency induce a dispersion of aggregate

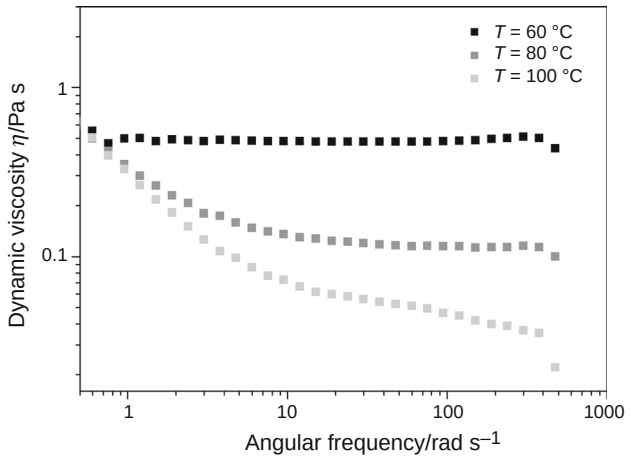

Fig. 8 Dynamic viscosity as a function of logarithmic angular frequency for the CNT-modified resin loaded at 1 mass% of MWCNT recorded at 60, 80, and 100 °C

network: The dynamic viscosity of the epoxy/1 mass% CNT composite decreases.

Conclusions

The polymerization and the rheological properties of a single-component epoxy resin RTM6 were studied for preheating and injection optimization. This commercial resin is used as unfilled in matrix composites for structural applications in the aeronautical industry. The differential scanning calorimetric analysis is used for description of the curing process under isothermal conditions at 80 °C. The polymerization evolution is studied through residual polymerization enthalpy and glass transition temperature evolutions. Three curing steps have been identified. The first one occurs between 0 and 10 h. Resin is a viscous liquid and there is no cross-linking reaction. During this time, the resin can be used without any risk of polymerization (storage, charges dispersion, injection). The second time range is between 10 and 55 h. The gel point is reached, the resin is in the rubbery state and the polymerization rate is fast. Finally, the third stage of polymerization begins at the vitrification after 55 h. The maximum conversion of the reactive groups is achieved. After 70 h, the RTM6 resin reaches a maximum conversion of 75 % for an isotherm of 80 °C. Physical aging phenomena are detected and induce a slight increase in the glass transition temperature.

Rheological behavior is investigated by a shear rheometer using a Couette geometry, particularly suitable for the study of low viscosity dispersions. Analysis by frequency sweeps from 0.06 to 500 rad s^{-1} showed that the resin has a Newtonian behavior over a wide frequency range, regardless of the temperature (60, 80, and 100 °C). A decrease in viscosity occurs beyond a critical angular pulsation whose value shifts with temperature. Finally, a reduction in viscosity is made possible by a rise of temperature. The integration of carbon nanotubes in the matrix increases the RTM6 dynamic viscosity at low frequencies. The rheological behavior depends on the CNTs concentration. At low concentration, the Newtonian plateau is observed. However, above a critical CNTs concentration, the resin becomes shear thinning. This transition is also observed for a specific CNTs fraction while varying the temperature. When the temperature increases, the resin loses its Newtonian behavior to become shear thinning. These phenomena can be explained by the formation of an interconnected CNT aggregates network which is broken under shear forces/stress.

RTM6 resin process parameters have been determined for a 80 °C isothermal temperature. When the resin is heated up to this recommended injection temperature, it can be used during 10 h before the activation of curing reactions. A frequency range for which the resin is described by a Newtonian rheological behavior has been determined. Modifications of this behavior due to resin formulation by CNTs introduction have been evaluated. The rise in induced CNTs introduction can be lowered by an increase in temperature or a high shear level.

References

1. Wang S, Chung DDL. Interlaminar interface in carbon fiber polymer-matrix. Compos Interfaces. 1998;6:497–505.
2. Iijima S. Helical microtubules of graphitic carbon. Nature. 1991;354:56–8.
3. Lonjon A, Demont P, Dantras E, Lacabanne C. Electrical conductivity improvement of aeronautical carbon fiber reinforced polyepoxy composites by insertion of carbon nanotubes. J Non-Cryst Solids. 2012;358:1859–62 Elsevier B.V.
4. Bauhofer W, Kovacs JZ. A review and analysis of electrical percolation in carbon nanotube polymer composites. Compos Sci Technol. 2009;69:1486–98 Elsevier Ltd.
5. Lux F. Review models proposed to explain the electrical conductivity of mixtures made of conductive and insulating materials. J Mater. 1993;28:285–301.
6. Barrau S, Demont P, Peigney A. DC and AC conductivity of carbon nanotubes-polyepoxy composites. Macromolecules. 2003;36:5187–94.
7. Gojny FH, Wichmann MHG, Fiedler B, Bauhofer W, Schulte K. Influence of nano-modification on the mechanical and electrical properties of conventional fibre-reinforced composites. Compos Part A Appl Sci Manuf. 2005;36:1525–35.
8. Qiu J, Zhang C, Wang B, Liang R. Carbon nanotube integrated multifunctional multiscale composites. Nanotechnology. 2007; 18:275708.
9. Zeng X, Yu S, Sun R. Effect of functionalized multiwall carbon nanotubes on the curing kinetics and reaction mechanism of bismaleimide–triazine. J Therm Anal Calorim. 2013;114:387–95 Springer Netherlands.

10. Gude MR, Prolongo SG, Ureña A. Effect of the epoxy/amine stoichiometry on the properties of carbon nanotube/epoxy composites. J Therm Anal Calorim. 2012;108:717–23 Springer Netherlands.
11. Schulz SC, Faiella G, Buschhorn ST, Prado LASA, Giordano M, Schulte K, et al. Combined electrical and rheological properties of shear induced multiwall carbon nanotube agglomerates in epoxy suspensions. Eur Polym J. 2011;47:2069–77 Elsevier Ltd.
12. Hexcel. HexFlow® RTM 6 Product Data [Internet]. http://www.hexcel.com/Resources/DataSheets/RTM-Data-Sheets/RTM6_global.pdf. Accessed 15 Apr 2014.
13. Skordos AA, Partridge IK. Determination of the degree of cure under dynamic and isothermal curing conditions with electrical impedance. J Polym Sci Part B Polym Phys. 2003;42:146–54.
14. Aduriz XA, Lupi C, Boyard N, Bailleul J-L, Leduc D, Sobotka V, et al. Quantitative control of RTM6 epoxy resin polymerisation by optical index determination. Compos Sci Technol. 2007;67:3196–201.
15. El Sawi I, Olivier PA, Demont P, Bougherara H. Investigation of the effect of double-walled carbon nanotubes on the curing reaction kinetics and shear flow of an epoxy resin. J Appl Polym Sci. 2012;126:358–66.
16. Karkanas PI, Partridge IK. Cure modeling and monitoring of epoxy/amine resin systems. I. Cure kinetics modeling. J Appl Polym Sci. 2000;77:1419–31.
17. Moosburger-Will J, Greisel M, Sause MGR, Horny R, Horn S. Influence of partial cross-linking degree on basic physical properties of RTM6 epoxy resin. J Appl Polym Sci. 2013;130:4339–46.
18. Mukherjee G. Evaluation of processing temperature in the production of fibre reinforced epoxy composites. J Therm Anal Calorim. 2012;108:947–50 Springer Netherlands.
19. Turi EA. Thermal characterization of polymeric materials. New York: Adcademic Press; 1997. p. 1396–418.
20. Pascault JP, Williams RJJ. Glass transition temperature versus conversion relationships for thermosetting polymers. J Polym Sci Part B Polym Phys. 1990;28:85–95 Wiley.
21. Kaelbe DH. Physical and chemical properties of cured resins. In: May CA, Tanaka Y, editors. Epoxy resins: chemistry and technology. New York: Marcel Dekker; 1973. p. 327–371.
22. Pascault J, Sautereau H, Verdu J, Williams R. Thermosetting polymers. Boca Raton: CRC Press; 2002.
23. Hutchinson JM. Interpretation of glass transition phenomena in the light of the strength-fragility concept. Polym Int. 1998;47:56–64.
24. Hutchinson JM. Physical aging of polymers. Prog Polym Sci. 1995;20:703–30.
25. Hutchinson JM, McCarthy D, Montserrat S, Cortés P. Enthalpy relaxation in a partially cured epoxy resin. J Polym Sci Part B Polym Phys. 1996;34:229–39 Wiley.
26. Odegard GM, Bandyopadhyay A. Physical aging of epoxy polymers and their composites. J Polym Sci Part B Polym Phys. 2011;49:1695–716 Wiley.
27. Fogel M, Parlevliet P, Geistbeck M, Olivier P, Dantras E. Thermal, rheological and electrical characterization of MWCNTs/epoxy matrices for an innovative spray process. Compos Sci Technol (Under revision).
28. Rahatekar SS, Koziol KKK, Butler SA, Elliott JA, Shaffer MSP, Mackley, et al. Optical microstructure and viscosity enhancement for an epoxy resin matrix containing multiwall carbon nanotubes. J Rheol. 2006;50:599 N. Y. N. Y.
29. Ma A, Chinesta F, Mackley M. The rheology and modeling of chemically treated carbon nanotubes suspensions. J Rheol. 2009;53:547 N. Y. N. Y.